

- [18] D.H. Hyun, M. Lee, N. Hattori, S. Kubo, Y. Mizuno, B. Halliwell, P. Jenner, Effect of wild-type or mutant parkin on oxidative damage, nitric oxide, antioxidant defenses, and the proteasome, *J. Biol. Chem.* 277 (2002) 28572–28577.
- [19] O. Corti, C. Hampe, H. Koutnikova, F. Darios, S. Jacquier, A. Prigent, J.C. Robinson, L. Pradier, M. Ruberg, M. Mirande, E. Hirsch, T. Rooney, A. Fournier, A. Brice, The p38 subunit of the aminoacyl-tRNA synthetase complex is a parkin substrate: linking protein biosynthesis and neurodegeneration, *Hum. Mol. Genet.* 12 (2003) 1427–1437.
- [20] H.S. Ko, R. von Coelln, S.R. Sriram, S.W. Kim, K.K. Chung, O. Pletnikova, J. Troncoso, B. Johnson, R. Saffary, E.L. Goh, H. Song, B.J. Park, M.J. Kim, S. Kim, V.L. Dawson, T.M. Dawson, Accumulation of the authentic parkin substrate aminoacyl-tRNA synthetase cofactor, p38/JTV-1, leads to catecholaminergic cell death, *J. Neurosci.* 25 (2005) 7968–7978.
- [21] S.Y. Kao, Regulation of DNA repair by parkin, *Biochem. Biophys. Res. Commun.* 382 (2009) 321–325.
- [22] N. Cohen, F. Muntoni, Multiple pathogenetic mechanisms in X linked dilated cardiomyopathy, *Heart* 90 (2004) 835–841.
- [23] A. Aartsma-Rus, A.A. Janson, W.E. Kaman, M. Bremmer-Bout, J.T. den Dunnen, F. Baas, G.J. van Ommen, J.C. van Deutekom, Therapeutic antisense-induced exon skipping in cultured muscle cells from six different DMD patients, *Hum. Mol. Genet.* 12 (2003) 907–909.
- [24] O.L. Gurvich, T.M. Tuohy, M.T. Howard, R.S. Finkel, L. Medne, C.B. Anderson, R.B. Weiss, S.D. Wilton, K.M. Flanigan, DMD pseudoexon mutations: splicing efficiency, phenotype, and potential therapy, *Ann. Neurol.* 63 (2008) 81–89.
- [25] J.C. van Deutekom, A.A. Janson, I.B. Ginjaar, W.S. Frankhuizen, A. Aartsma-Rus, M. Bremmer-Bout, J.T. den Dunnen, K. Koop, A.J. van der Kooi, N.M. Goemans, S.J. de Kimpe, P.F. Ekhart, E.H. Venneker, G.J. Platenburg, J.J. Verschuuren, G.J. van Ommen, Local dystrophin restoration with antisense oligonucleotide PRO051, *N. Engl. J. Med.* 357 (2007) 2677–2686.
- [26] S. Asakawa, N. Hattori, A. Shimizu, Y. Shimizu, S. Minoshima, Y. Mizuno, N. Shimizu, Analysis of eighteen deletion breakpoints in the parkin gene, *Biochem. Biophys. Res. Commun.* 389 (2009) 181–186.

# Protein kinase C $\gamma$ , a protein causative for dominant ataxia, negatively regulates nuclear import of recessive-ataxia-related aprataxin

Hirohide Asai<sup>1</sup>, Makito Hirano<sup>1,\*</sup>, Keiji Shimada<sup>2</sup>, Takao Kiriya<sup>1</sup>, Yoshiko Furiya<sup>1</sup>, Masanori Ikeda<sup>1</sup>, Takaaki Iwamoto<sup>3</sup>, Toshio Mori<sup>3</sup>, Kazuto Nishinaka<sup>4</sup>, Noboru Konishi<sup>2</sup>, Fukushi Uda<sup>4</sup> and Satoshi Ueno<sup>1</sup>

<sup>1</sup>Department of Neurology, <sup>2</sup>Department of Pathology and <sup>3</sup>Radioisotope Research Center, Nara Medical University School of Medicine, 840 Shijo-cho, Kashihara, Nara 634-8522, Japan and <sup>4</sup>Department of Neurology, Sumitomo Hospital, Osaka, Japan

Received March 24, 2009; Revised and Accepted June 24, 2009

Spinocerebellar ataxia type 14 (SCA14) is an autosomal dominant disease caused by mutations in the gene encoding protein kinase C $\gamma$  (PKC $\gamma$ ). We report an SCA14 family with a novel deletion of a termination-codon-containing region, resulting in a missense change and a C-terminal 13-amino-acid extension with increased kinase activity. Notably, one patient with a severe phenotype is the first homozygote for the mutation causing SCA14. We show the novel molecular consequences of increased kinase activities of mutants: aprataxin (APTX), a DNA repair protein causative for autosomal recessive ataxia, was found to be a preferential substrate of mutant PKC $\gamma$ , and phosphorylation inhibited its nuclear entry. The phosphorylated residue was Thr111, located adjacent to the nuclear localization signal, and disturbed interactions with importin  $\alpha$ , a nuclear import adaptor. Decreased nuclear APTX increased oxidative stress-induced DNA damage and cell death. Phosphorylation-resistant APTX, kinase inhibitors, and antioxidants may be therapeutic options for SCA14.

## INTRODUCTION

Spinocerebellar ataxia type 14 (SCA14) is an autosomal dominant cerebellar ataxia, associated with various combinations of myoclonus, parkinsonism and dementia. Causative mutations have been identified in the *PRKCG* gene encoding protein kinase C $\gamma$  (PKC $\gamma$ ). PKC $\gamma$ , comprising 697 amino acids with two N-terminal regulatory and two C-terminal catalytic domains, is a major PKC isoform in cerebellar Purkinje cells and regulates certain motor learning functions and cell morphology (1). SCA14 mutations occur outside of essential catalytic sites, and all tested mutants retain kinase activities (2). A reported out-of-frame splice-site mutation (D95D) may be a benign, splicing-unaffected polymorphism (3), since it has been found in an expression sequence tag database (NCBI accession #DC319291 and EL734626). Collectively, retained mutant activities may be critical to the pathomechanism of SCA14.

Previous studies proposed several contradictory pathomechanisms of SCA14, such as haploinsufficiency (loss of half of kinase activity), dominant negative effects of mutants, or gain of toxic function, including increased kinase activities and aggregation formation (2,4–6). Moreover, how these properties lead to cell death remains controversial: endoplasmic reticulum (ER) stress and disturbed Ca<sup>++</sup> homeostasis may be involved (5,7). Given that several mutants have no obvious cytotoxicity in normal cell cultures, pathomechanisms of SCA14 probably involve other additional factors, such as oxidative stress, implicated in many neurodegenerative diseases. Addressing these issues is essential for the identification of pathways capable of being targeted therapeutically.

To explore common pathological pathways involved in various hereditary ataxias, extensive effort has been put into the establishment of interaction networks for ataxia-related proteins (8). Such efforts, however, have failed to identify

\*To whom correspondence should be addressed. Tel: +81 744298860; Fax: +81 744246065; Email: hirano\_makito@yahoo.co.jp or mhirano@narmed-u.ac.jp

ataxia-related PKC $\gamma$  substrates. In contrast, a number of proteins that are not directly associated with ataxia or Purkinje cell loss have been identified as PKC $\gamma$  substrates, such as metabotropic glutamate receptor 5, non-muscle myosin heavy chain II-B, myristoylated alanine-rich C kinase substrate (MARCKS), GSP43/B-50, HMG-I, RC3/neurogranin and glycogen synthetase (9–13). Nevertheless, accumulating evidence that either increased or decreased PKC $\gamma$  activity affects Purkinje cell function suggests the presence of ataxia-related substrates (14). Identification of new substrates may clarify the pathogenic roles of mutant PKC $\gamma$  in known cellular pathways involving identified proteins.

In this study, we report an SCA14 family with a new type of mutation, i.e. a deletion of a termination-codon-containing region of the *PRKCG* gene, producing a mutant PKC $\gamma$  protein (M697Iex) with a missense change (M697I) and a C-terminal 13-amino-acid extension (Ext13) with increased kinase activity. Notably, one patient with a severe phenotype is the first homozygote for the mutation causing SCA14. Our findings shed new light on the molecular consequences of increased kinase activities of PKC $\gamma$  mutants: aprataxin (APT $\alpha$ ), a DNA repair protein causative for autosomal recessive ataxia, was found to be a preferential substrate for mutant PKC $\gamma$ , and the resultant phosphorylation inhibited its nuclear entry because of disturbed interactions with importin  $\alpha$ , a nuclear import adaptor. Decreased nuclear APT $\alpha$  sensitized cells to oxidative stress by increasing unrepaired DNA damage. Phosphorylation-resistant APT $\alpha$ , a kinase inhibitor, and antioxidants reduced DNA damage and thus cell death.

## RESULTS

### Identification of a new mutation

PCR and sequence analysis of the *PRKCG* gene and mRNA revealed that the proband (Patient 1) was homozygous and her paternal grandmother (Patient 2) was heterozygous for a novel 102 bp deletion including the termination codon in exon 18 (Fig. 1A and B). No other mutation was detected. This deletion resulted in an amino acid change from the phylogenetically conserved Met to Ile at the 697 codon and an extension of 13 amino acids (M697Iex). Two hundred control subjects lacked this mutation. These results suggested that the parents of the proband were obligate heterozygotes who remained asymptomatic at the ages of 49 and 45 years. Because the age at onset in Patient 2 was 60 years, symptoms of heterozygotes would presumably develop later in life.

### Confirmation of *PRKCG* gene homozygosity and stable mRNA

We quantified exon 18 of the *PRKCG* gene in genomic DNA of the proband and found that the patient had two copies of exon 18 (Fig. 1C). RT-PCR with primers on exon 17–18 showed that the mutant transcript was expressed in Patients 1 and 2 (Fig. 1D, left panel). Possible mRNA instability or transcriptional inactivation was excluded by the fact that the amount of total PKC $\gamma$  cDNA in the patients was equivalent to that in a sex-matched control on quantitative RT-PCR with primers on exon 11–12 (Fig. 1D, right panel), which

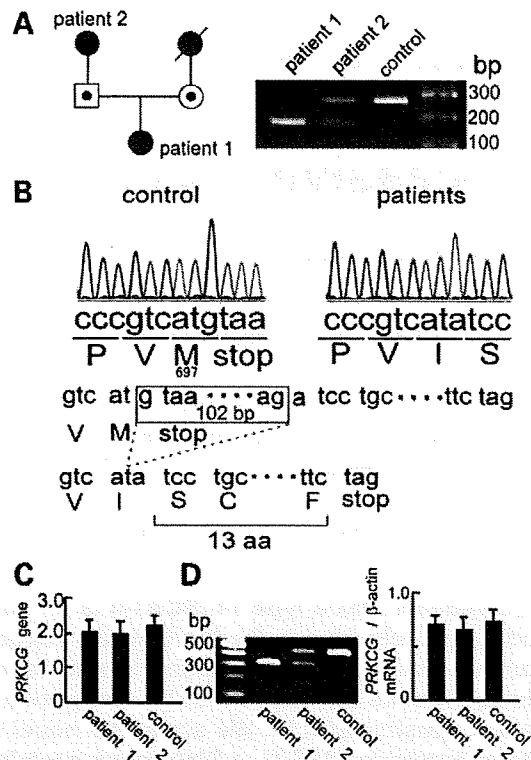


**Figure 1.** Analyses of the *PRKCG* gene and mRNA. (A) A family tree of the index family (left). Gene analyses were performed only for Patients 1 and 2. The parents of Patient 1 were obligate carriers. The maternal grandmother (hatched symbol) had late-onset parkinsonism; detailed medical records were unavailable. PCR-amplification of exon 18 in the *PRKCG* gene showed that both patients had a band shorter than a control band (right). Patient 1 was homozygous and Patient 2 was heterozygous for this potential deletion mutation. (B) Sequence analysis of the shorter band revealed a 102 bp deletion in the 3'-region, resulting in a novel mutant protein (M697Iex) bearing a missense change from Met to Ile at the 697 codon and a 13-amino-acid extension. (C) Real-time PCR of genomic DNA showed that both patients had two copies of the *PRKCG* gene. (D) RT-PCR with primers on exons 17 and 18 showed that Patient 1 had the only mutant transcript and Patient 2 had both normal and mutant ones (left panel). Real-time RT-PCR with primers on exons 11 and 12 revealed no significant differences in total *PRKCG* mRNA levels between control subjects and patients (right panel). The bar represents the mean  $\pm$  SD from five independent experiments.

was confirmed in five additional control individuals (data not shown). Equivalent mRNA expression from wild-type (WT) and mutant alleles in Patient 2 was confirmed by the WT or mutant-specific real-time PCR method using primers on exon 18 (data not shown).

### Increased kinase activities of mutants

Immunoblot confirmed that the amounts of GFP-tag and untagged mutant PKC $\gamma$  proteins expressed in human neuroblastoma SH-SY5Y cells did not differ significantly from those of WT PKC $\gamma$  (Supplementary Material, Fig. S1), with equivalent exogenous *PRKCG* mRNA levels (data not shown), indicating that the mutant proteins were not highly unstable. Kinase assay of GFP-PKC $\gamma$  purified by immunoprecipitation showed that kinase-dead (KD) proteins had lost activities but that all other mutants had significantly higher

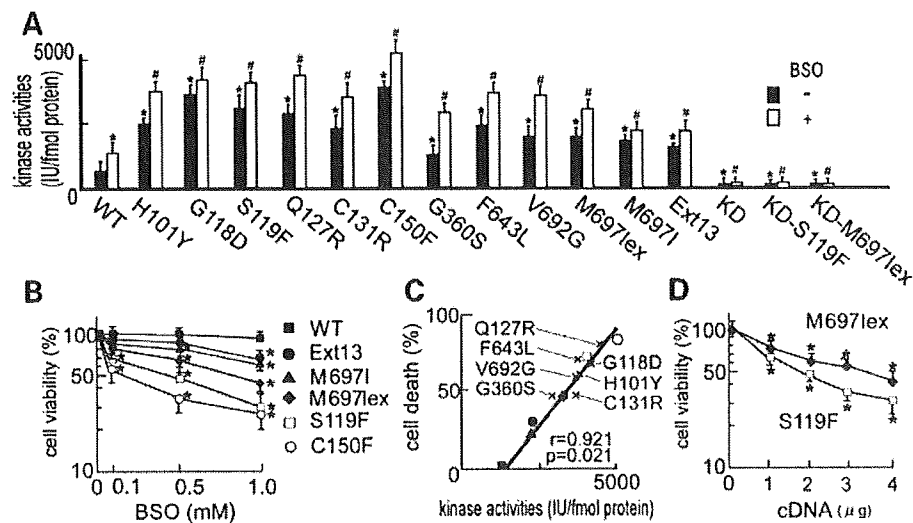


**Figure 2.** Kinase activities of various types of PKC $\gamma$  and hypersusceptibility to oxidative stress in SH-SY5Y cells expressing mutant PKC $\gamma$ . (A) Kinase activities of various PKC $\gamma$  proteins with or without oxidative stress. After transfection of SH-SY5Y cells with WT or mutant GFP-PKC $\gamma$  cDNAs, cells were treated with or without 1 mM BSO, an oxidative-stress inducer, for 12 h, without cell death. GFP-PKC $\gamma$  protein was immunoprecipitated from cell lysates. KD mutants almost completely lost their activities. All other mutants had significantly higher activities than WT. BSO increased activities in both WT and mutants. The bar represents the mean  $\pm$  SD from five independent experiments. \* $P < 0.05$ , unpaired Student's  $t$ -test as compared with the sample for WT transfection without BSO treatment. # $P < 0.05$ , unpaired Student's  $t$ -test as compared with the sample for WT transfection with BSO treatment. (B) SH-SY5Y cells transfected with plasmids encoding WT or representative mutant PKC $\gamma$  were treated with BSO for 24 h. Cell survival assay revealed that the viability of cells expressing mutant PKC $\gamma$  but not WT was reduced in a BSO-dependent manner. The bar represents the SD from five independent experiments. \* $P < 0.01$ , Mann-Whitney  $U$  test as compared with no BSO treatment. (C) The kinase activities of mutant and WT PKC $\gamma$  significantly correlated with the ratios of cell death caused by 1 mM BSO treatment. The figure symbols are the same as in (B). (D) SH-SY5Y cells were transfected separately with 0–4  $\mu$ g of M697lex and S119F PKC $\gamma$  plasmid, and treated with 1 mM BSO for 24 h. M697lex and S119F mutant dose-dependently reduced cell viability. The bar represents the SD from five independent experiments. \* $P < 0.01$ , Mann-Whitney  $U$  test as compared with mock transfection.

activities than WT (Fig. 2A). A previous report described that G360S and V692G mutants had decreased activity and activity equivalent to WT PKC $\gamma$ , respectively (15). The discrepancy between the present and previous results may be explained by the difference in the cells used, i.e. monkey kidney COS7 cells in the previous study and human neuroblastoma cells in this study. The activities in our experiment were increased by treatment with L-buthionine-(S,R)-sulfoximine (BSO), an oxidative stress inducer. BSO inhibits synthesis of glutathione, a free-radical scavenger, and thus increases endogenous reactive oxygen species (ROS). The activity of M697lex was higher than that of M697I or Ext13.

Cotransfection of mutants and WT showed simply additive effects, rather than dominant negative effects (Supplementary Material, Fig. S2). Simple additions of the anti-PKC $\gamma$  antibody used previously for immunoprecipitation to our assay system dose-dependently suppressed the kinase activities of WT and mutant PKC $\gamma$  (Supplementary Material, Fig. S3), suggesting that activities might be further suppressed by immunoprecipitation with this antibody (16,17). Unrelated antibodies, including anti-actin antibody and anti-GFP-antibody, did not affect activity (data not shown).

A similar but mild increase in kinase activities using the endogenous substrate MARCKS was provided by mutant PKC $\gamma$  (S119F and M697lex) under oxidative stress as compared with that by the WT (Supplementary Material, Fig. S4). This result, however, was inconsistent with the previous finding that mutants showed reduced phosphorylation of MARCKS (18), possibly because different cell lines were

used, i.e. uterine epithelial cancer HeLa cells in the previous study and neuroblastoma SH-SY5Y cells in the present study.

#### Hypersensitivity of cells expressing mutant PKC $\gamma$ to oxidative stress

We cultured human neuroblastoma SH-SY5Y cells transfected with WT and mutant PKC $\gamma$  cDNAs in a medium with BSO. In this model of oxidative stress, the endogenous formation of ROS is largely unopposed, consequently resulting in oxidative cell damage (19). Treatment with 1 mM BSO for 24 h decreased the viability of cells with mutant PKC $\gamma$  to 30–70% of the base-line level, but did not affect that of cells with WT-PKC $\gamma$  (Fig. 2B) or KD-PKC $\gamma$  (not shown). Cell death, characterized by chromatin condensation and loss of propidium iodide exclusion (data not shown), started after 18-h incubation with BSO. Linear regression analysis showed that the kinase activities were positively associated with the cell death ratios under oxidative stress (Fig. 2C). Cell viability was reduced by increasing the amounts of transfected M697lex and S119F mutant cDNAs (Fig. 2D).

#### Decreased nuclear accumulation of APTX and interaction of APTX and PKC $\gamma$

To find PKC $\gamma$  substrates implicated in the pathomechanism of SCA14, we searched neurodegeneration-associated proteins and various nuclear proteins whose physiological localization was affected by mutant PKC $\gamma$  in live SH-SY5Y cells, since

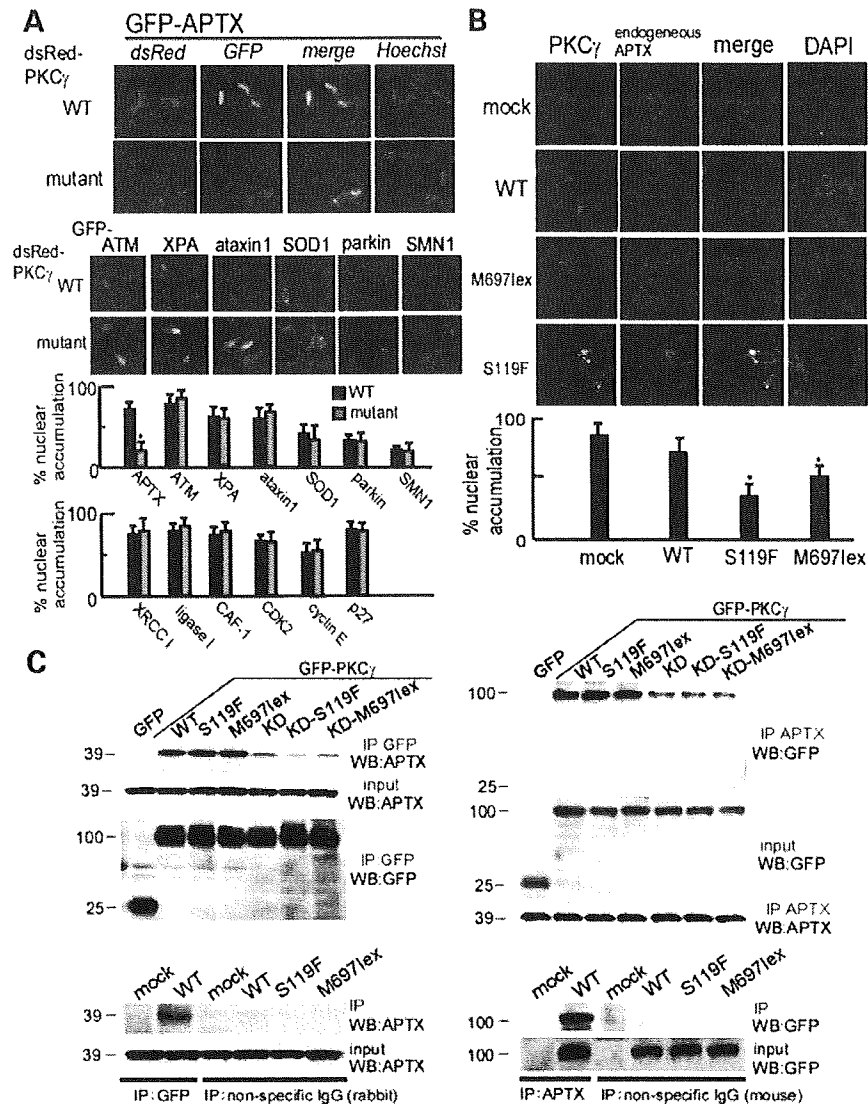


**Figure 3.** Impaired nuclear localization of APTX by mutant PKC $\gamma$  and interaction of these proteins. (A) Coexpression of WT or the common mutant S119F-dsRed-PKC $\gamma$  with various GFP-fused proteins in SH-SY5Y cells. The upper panels (fluorescent images and a graph) show APTX and other neurodegenerative disease-causing proteins, although the lower panel (a graph) shows nuclear proteins. Nuclear accumulations of GFP-APT $\gamma$  were significantly lower in cells expressing S119F-PKC $\gamma$  than in WT-PKC $\gamma$  transfection cells, whereas other GFP-fused proteins showed similar localization patterns in both WT and S119F-PKC $\gamma$  transfection cells. \* $P < 0.05$ , unpaired Student's  $t$ -test as compared with WT transfection cells. (B) Effects of mutant (S119F and M697lex) PKC $\gamma$  on endogenous APTX. SH-SY5Y cells were separately transfected with WT-, S119F- and M697lex-GFP-PKC $\gamma$  plasmids. Endogenous APTX was immunostained with anti-APT $\gamma$  monoclonal antibody and Alexa594-secondary antibody (red). Nuclear accumulation of APTX was reduced in cells expressing mutant PKC $\gamma$ , but not WT-PKC $\gamma$ . The bar represents the mean  $\pm$  SD from five independent experiments. \* $P < 0.05$ , unpaired Student's  $t$ -test as compared with mock transfection cells. (C) Interaction of WT/mutant PKC $\gamma$  and endogenous APTX. Immunoprecipitation (IP) with anti-GFP antibody followed by western blot (WB) with anti-APT $\gamma$  and anti-GFP antibodies showed interaction of endogenous APTX with WT/mutant GFP-PKC $\gamma$  expressed in SH-SY5Y cells (upper left panels). The converse experiment confirmed the results (upper right panels). KD PKC $\gamma$  proteins considerably decreased the interaction. Nonspecific interactions of endogenous APTX or GFP-PKC $\gamma$  with rabbit or mouse IgG were excluded by IP with nonspecific IgG (lower panels).

a very recent study demonstrates that PKC $\gamma$  inhibits nuclear import of a possible substrate (20). A fluorescent microscope-based quantitative analysis, as described previously (19), for nuclear localization of proteins coexpressed with mutant PKC $\gamma$  revealed that only nuclear accumulation of APTX was impaired (Fig. 3A). In contrast, nuclear localization was not altered in other proteins, such as neurodegenerative disease-causing [ataxia telangiectasia mutated (ATM),

Xeroderma pigmentosum Group A (XPA), ataxin1, superoxide dismutase 1 (SOD1), parkin and survival motor neuron 1 (SMN1)]. DNA-repair [XRCC1, DNA ligase I, and chromatin assembly factor 1 (CAF-1)], and cell cycle-related proteins [cyclin dependent kinase 2 (CDK2), cyclin E and p27/Kip1]. The main subcellular localizations of SOD1 (cytoplasm), parkin (ER) and SMN1 (cytoplasm and nucleus) were also unaltered. The nuclear accumulation of endogenous APTX

was also decreased by S119F and M697Iex mutant PKC $\gamma$  (Fig. 3B). Immunoprecipitation studies confirmed that WT and mutant PKC $\gamma$  proteins interacted with WT-APT $\chi$  (Fig. 3C), which is prerequisite for APT $\chi$  to be a substrate of PKC $\gamma$ . A control experiment using nonspecific IgG showed no interaction between IgG and APT $\chi$ /PKC $\gamma$ .

#### Interaction of PKC $\gamma$ with APT $\chi$ , and phosphorylation of APT $\chi$ at Thr111

To confirm phosphorylation of APT $\chi$  and identify a phosphorylation site, threonine and/or serine residues near the nuclear localization signal in APT $\chi$  (Thr111 and Ser118) were mutagenized to phosphorylation-resistant alanine. *In vitro* kinase assay showed that the Km, kcat and kcat/Km (the catalytic efficiency of the enzyme) values, using recombinant WT-APT $\chi$  substrate, were, respectively,  $155.0 \pm 14.3 \mu\text{M}$ ,  $8.2 \pm 1.0 \text{ min}^{-1}$ , and  $52.9 \pm 6.5 \text{ mM}^{-1} \text{ min}^{-1}$  (mean  $\pm$  SD) for WT-PKC $\gamma$ ,  $38.2 \pm 8.2 \mu\text{M}$ ,  $5.4 \pm 0.4 \text{ min}^{-1}$ , and  $141.4 \pm 10.5 \text{ mM}^{-1} \text{ min}^{-1}$  for S119F, and  $80.6 \pm 7.5 \mu\text{M}$ ,  $6.2 \pm 0.4 \text{ min}^{-1}$ , and  $76.9 \pm 5.0 \text{ mM}^{-1} \text{ min}^{-1}$  for M697Iex. These measures were unobtainable for the substrate T111A-APT $\chi$  because of too little phosphorylation. Polyacrylamide gel electrophoresis of end products after sufficient incubation to allow complete phosphorylation of various types of recombinant-APT $\chi$  showed that WT- and S118A-APT $\chi$ , but not T111A-APT $\chi$ , were phosphorylated by both WT- and mutant (S119F and M697Iex) PKC $\gamma$  (Fig. 4A). Phosphorylation at Thr111 was confirmed by the experiment using the synthetic peptides, excluding the possibility that Thr111 is a phosphorylation-permitted residue, i.e. a site that is not phosphorylated itself but permits near-by phosphorylation. The immunocytochemical analysis showed reduced nuclear accumulation of WT- and S118A-APT $\chi$ , but not of T111A-APT $\chi$  in the presence of mutant PKC $\gamma$  (Fig. 4B). KD-S119F-PKC $\gamma$  failed to affect the nuclear import. Partly impaired nuclear import was found in phosphomimetic T111E-APT $\chi$  without PKC $\gamma$ , presumably because the one increased negative charge of glutamate in T111E ( $-\text{COO}^-$ ) is smaller than the three negative charges induced by phosphorylation ( $-\text{PO}_4^{3-}$ ). The PKC specific inhibitor calphostin C restored impaired nuclear import of APT $\chi$ . The results of *in vivo* phosphorylation in SH-SY5Y cells, subcellular fractionation, and immunoprecipitation showed that GFP-WT-APT $\chi$  was phosphorylated profoundly by mutant (S119F and M697Iex) PKC $\gamma$  and mildly by WT-PKC $\gamma$  and was present in the cytoplasm (Fig. 4C). In contrast, GFP-T111A-APT $\chi$  was not phosphorylated and was present in the nucleus. Mutant PKC $\gamma$  (S119F and M697Iex) phosphorylated WT-APT $\chi$  considerably more than did WT-PKC $\gamma$ . Calphostin C inhibited phosphorylation and promoted nuclear entry of WT-APT $\chi$ . Collectively, phosphorylation occurred at Thr111, reducing nuclear APT $\chi$ .

#### Phosphorylation at Thr111 inhibited interaction of APT $\chi$ with importin $\alpha$

Importin  $\alpha$  is an adaptor that facilitates nuclear import of APT $\chi$  and other proteins bearing a classic nuclear localization signal. Unphosphorylated and/or phosphorylated dsRed-APT $\chi$  by mutant (S119F and M697Iex) PKC $\gamma$  expressed in

SH-SY5Y cells was immunoprecipitated with anti-APT $\chi$  monoclonal antibody and subjected to western blot with anti-importin  $\alpha$  and anti-APT $\chi$  antibodies. Conversely, importin  $\alpha$  was immunoprecipitated, and APT $\chi$  and importin  $\alpha$  were detected by western blot (data not shown). The results showed that unphosphorylated WT-APT $\chi$  and phosphorylation-resistant T111A-APT $\chi$  interacted with importin  $\alpha$  (Fig. 4D). In contrast, phosphorylated WT-APT $\chi$  and S118A-APT $\chi$  considerably reduced and phosphomimetic T111E-APT $\chi$  mildly reduced interactions of APT $\chi$  with importin  $\alpha$ .

#### Restoration of DNA damage and cell death caused by mutant PKC $\gamma$ with a kinase inhibitor, antioxidants and expression of phosphorylation-resistant APT $\chi$

SH-SY5Y cells were transfected with plasmids encoding dsRed-APT $\chi$ /untagged LacZ and/or untagged mutant PKC $\gamma$  and cultured overnight. After 10-h treatment with 1 mM BSO (without cell death), cells were fixed briefly in 4% paraformaldehyde, immunostained with anti-7,8-dihydro-8-oxoguanine (8-oxoG) monoclonal antibody (19), and analyzed with the use of a fluorescence microscope. Expression of WT-APT $\chi$  alone reduced immunostained 8-oxoG, induced by BSO (Fig. 5A). Coexpression of mutant (S119F and M697Iex) PKC $\gamma$  reduced nuclear WT-APT $\chi$  and increased 8-oxoG, both of which were restored by the kinase inhibitor calphostin C. The coenzyme Q<sub>10</sub>-derivative antioxidant decylubiquinone (DEC) did not revert impaired nuclear accumulation of APT $\chi$ , but decreased 8-oxoG, suggesting that reduced oxidative stress cannot block phosphorylation of APT $\chi$  by mutant PKC $\gamma$ , but that even a small amount of nuclear APT $\chi$  may be adequate to deal with the reduced DNA damage after treatment with DEC. Phosphorylation-resistant T111A mutation reduced DNA damage, presumably because T111A-APT $\chi$  retained catalytic activity due to an intact active site (101% of WT) (21). Consistently, cell death was also reduced by T111A-APT $\chi$  transfection as well as by calphostin C treatment (Fig. 5B and C). The involvement of reduced APT $\chi$  in oxidative-stress-induced cell death was also supported by BSO-hypersensitivity of SH-SY5Y cells with an siRNA-mediated reduction in endogenous APT $\chi$  (data not shown). Antioxidants also contributed to cell survival. In contrast, cotransfection of parkin or treatment with z-ATAD-fink, an ER-stress blocker, did not affect cell survival.

#### Abundant cytoplasmic APT $\chi$ in Purkinje cells

Both conventional and fluorescent staining methods showed that Purkinje cells of control cerebellum had relatively high levels of APT $\chi$  and PKC $\gamma$ , as compared with granular neurons (Fig. 6A). APT $\chi$  was localized in both the cytoplasm and nucleus of Purkinje cells, which was further confirmed by immunostaining with another line (A3) of monoclonal anti-APT $\chi$  antibody (data not shown). Although PKC $\gamma$  was primarily localized in the cytoplasm, it was present partially in the nucleus, which seems at least partly consistent with a previous finding in rats (22). These results were essentially reproduced in two additional control brains (data not shown). In contrast, a previous finding from a single patient



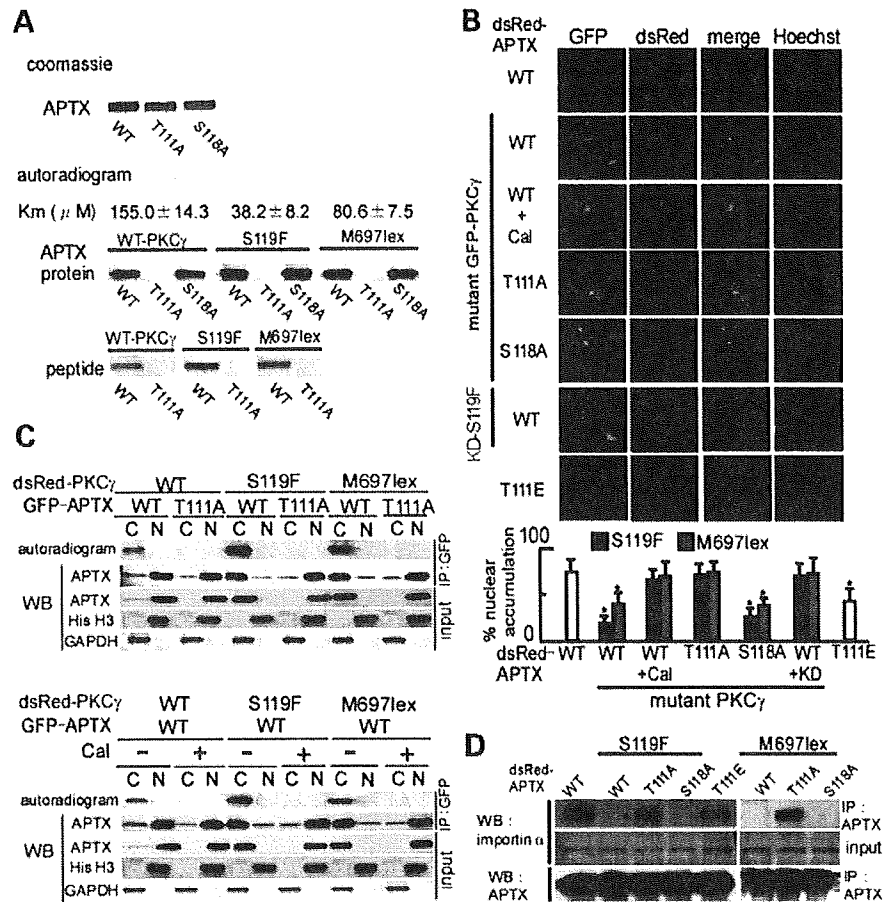


**Figure 4.** Identification of a phosphorylated residue of APTX and the mechanism inhibiting its nuclear entry. (A) Coomassie blue staining showed equivalent amounts of WT-, T111A- and S118A-APTX used as substrates for *in vitro* kinase assay (upper panel). Km values of WT- and mutant (S119F and M697lex) PKC $\gamma$ , using recombinant WT-APTX substrate, are shown above the autoradiographic images. Autoradiograms of the electrophoresed end products after complete phosphorylation revealed that both WT- and mutant (S119F and M697lex) PKC $\gamma$  phosphorylated WT- and S118A-APTX, but not T111A-APTX (middle panels). Similarly, phosphorylation of peptides around the Thr111 without Ser118 residue was seen in WT-APTX, but not in T111A-APTX (lower panel). (B) WT-dsRed-APTX was localized to the DAPI-stained nuclei in SH-SY5Y cells without PKC $\gamma$  expression, but was localized to the cytoplasm in S119F-GFP-PKC $\gamma$  transfected cells. The decreased nuclear accumulations of APTX were restored by calphostin C (Cal), a selective PKC inhibitor. S118A-APTX, but not T111A mutant, showed nuclear import failure in S119F-PKC $\gamma$  transfected cells. T111E-APTX, mimicking phosphorylated APTX, reduced nuclear import without PKC $\gamma$  expression. KD-S119F PKC $\gamma$  did not affect the nuclear import. M697lex had slightly mild effects on APTX nuclear accumulation, as shown in the graph. The bar represents the mean  $\pm$  SD from five independent experiments. \**P* < 0.05, unpaired Student's *t*-test as compared with the sample for WT-APTX transfection alone. (C) *In vivo* phosphorylation of APTX in SH-SY5Y cells. WT- and T111A-GFP-APTX plasmids were separately cotransfected with WT-, S119F- or M697lex-dsRed-PKC $\gamma$  plasmid, and were labeled with [<sup>32</sup>P]phosphate. Cytoplasmic (C) and nuclear (N)-fractionated and immunoprecipitation (IP)-purified proteins were subjected to autoradiography and western blotting (WB). WT-APTX was phosphorylated and present in the cytoplasm, although T111A-APTX was not phosphorylated and was present in the nucleus (upper panels). Mutant PKC $\gamma$  (S119F and M697lex) phosphorylated WT-APTX considerably more than did WT-PKC $\gamma$ . Calphostin (Cal) inhibited phosphorylation and promoted nuclear entry of WT-APTX. (D) Impaired interaction between phosphorylated APTX and the nuclear import adaptor importin  $\alpha$ . Immunoprecipitation assay showed that importin  $\alpha$  interacted with unphosphorylated WT-APTX and phosphorylation-resistant T111A-APTX, but had significantly reduced interactions with WT- and S118A-APTX phosphorylated by mutant (S119F and M697lex) PKC $\gamma$  and a mildly reduced interaction with phosphomimetic T111E-APTX.

with SCA14 showed that PKC $\gamma$  as well as ataxin1 was reduced in cerebellar Purkinje cells (14). However, ataxin1 mutation, known to suppress PKC $\gamma$  levels in ataxin1-transgenic mice, was not specified in this particular case because DNA analysis was not performed. In addition, because the time between death and tissue fixation could not be established, the reported reduction in PKC $\gamma$  might be attributed to post-mortem degradation. However, firm conclusions must await further studies.

### Cytoplasmic localization of APTX during neuronal differentiation in pheochromocytoma 12 cells

To monitor subcellular localization of APTX during neuronal differentiation with or without BSO-mediated oxidative stress, rat pheochromocytoma 12 (PC12) cells were used, since all-*trans*-retinol, a drug for differentiation of SH-SY5Y, functions as an antioxidant and blunts the effects of BSO. PC12 cells were differentiated with nerve growth factor and were

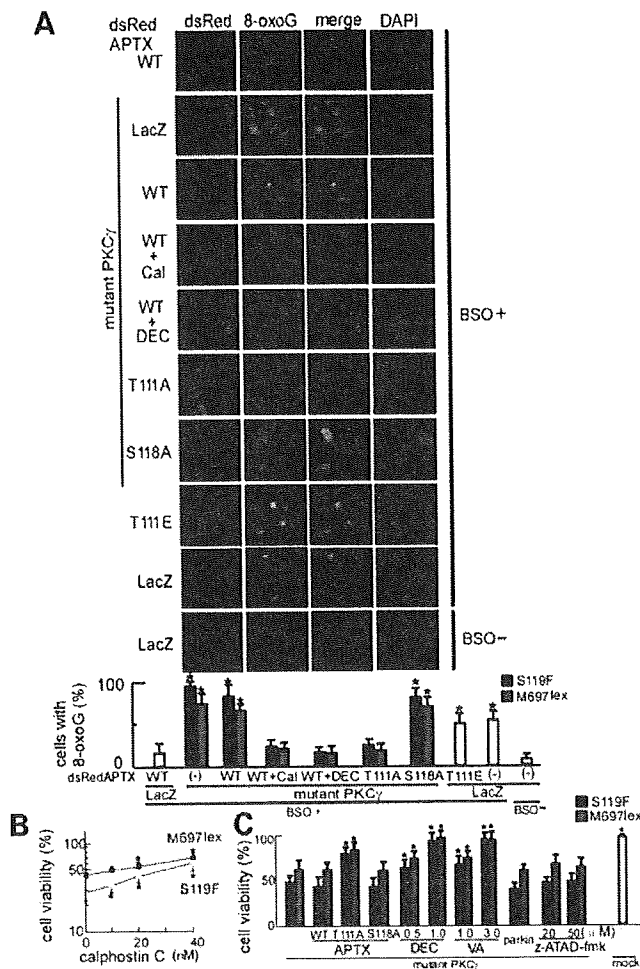


**Figure 5.** Effects of APTX phosphorylation on DNA damage and cell death. (A) DNA damage in SH-SY5Y cells expressing mutant PKC $\gamma$  and effects of various APTX mutants. Cells were transfected with dsRed-WT/T111A/T111E/S118A-APTX/LacZ gene [APT $\gamma$ (-)] with or without untagged mutant (S119F) PKC $\gamma$  cDNA, and treated with 1 mM BSO for 10 h, without cell death. An oxidatively damaged nucleotide (8-oxoguanine: 8-oxoG) was immunostained and visualized with FITC (green). Cells with reduced nuclear localization of WT- and S118A-APT $\gamma$  with mutant PKC $\gamma$  showed nuclear accumulation of 8-oxoG. T111E without mutant PKC $\gamma$  mildly reduced nuclear APTX and increased 8-oxoG. Treatment with the kinase inhibitor calphostin C (Cal) increased nuclear APTX and reduced 8-oxoG. In contrast, treatment with the antioxidant decylubiquinone (DEC) did not affect APTX localization, but reduced 8-oxoG. M697lex had milder effects on 8-oxoG accumulation as shown in the graph. The bar represents the mean  $\pm$  SD from five independent experiments. \* $P$  < 0.05, unpaired Student's  $t$ -test as compared with a sample for dsRed-WT-APT $\gamma$  transfection and BSO-treatment. (B) Calphostin C dose-dependently blocked cell death caused by 1 mM BSO for 24 h in SH-SY5Y cells expressing M697lex and S119F mutant PKC $\gamma$ . \* $P$  < 0.01, Mann-Whitney  $U$  test as compared with no calphostin C treatment. (C) BSO-induced cell death for mutant (S119F and M697lex) PKC $\gamma$  expression was also blocked by coexpression of phosphorylation-resistant T111A-APT $\gamma$  and by treatments with antioxidants (DEC and all-*trans*-retinol [VA]), but not by WT or S118A-APT $\gamma$  or by parkin expression. Treatment with the caspase 12 inhibitor z-ATAD-fmk had also no effect on cell viability. \* $P$  < 0.01, Mann-Whitney  $U$  test as compared with expression of mutant (S119F or M697lex) PKC $\gamma$  alone.

treated with or without 1 mM BSO. Differentiated cells treated with BSO were further treated with or without calphostin C. Endogenous WT-APT $\gamma$  was localized in the nuclei of

undifferentiated PC12 cells (Fig. 6B). BSO did not affect APT $\gamma$  localization, suggesting that endogenous WT-PKC $\gamma$  activated by BSO in undifferentiated PC12 cells was insufficient to phosphorylate APTX. In differentiated PC12 cells, APTX became localized in both cytoplasm and nuclei. Nuclear APTX was further decreased by transfection-induced dsRed-M697lex expression and by BSO treatment. The kinase inhibitor calphostin C increased nuclear APTX. Western blot showed that APTX also increased in differentiated PC12 cells, but the increment was smaller than that of PKC $\gamma$  (Fig. 6C). These results indicated that the cytoplasmic distribution of APTX in differentiated PC12 cells was at least partly due to increased PKC $\gamma$  expression.

**Aggregation of PKC $\gamma$**

Various PKC $\gamma$  cDNAs were transfected into SH-SY5Y cells, and aggregation was assessed under a fluorescent microscope. Consistent with previous findings (2,7), aggregation was much more frequent in cells with mutant PKC $\gamma$  (Supplementary Material, Fig. S5). Calphostin C treatment and KD-mutant PKC $\gamma$  proteins considerably reduced aggregation.

**DISCUSSION**

We here provide clinical and experimental evidence that mutant PKC $\gamma$  had dose-dependent toxicity, primarily associated with increased kinase activities. Mutants preferentially phosphorylated APTX, a DNA repair protein causative for autosomal recessive ataxia, inhibited nuclear import of APTX, and thus sensitized cells to oxidative stress-induced DNA damage, leading to cell death.

**Dose-, mutant- and oxidative-stress-dependent increases in kinase activity of mutant PKC $\gamma$**

The novel mutant protein (M697lex) had increased kinase activity, attributed additively to a missense change and a sequence extension. We speculate that a presumed 2-fold increase in activity in the homozygote leads to earlier disease onset than in heterozygotes. This possible clinical dosage effect was supported by experimental dose-dependent toxicities of M697lex and the common mutant S119F. Notably, the mutant toxicities seemed to parallel the increased kinase activities *in vitro*. In contrast, dominant-negative effects of mutants suggested previously seem unlikely in our family, since the homozygote lacked WT protein to be inhibited. In addition, no dominant negative effects were observed experimentally (Supplementary Material, Fig. S2). This mechanism potentially leading to loss of PKC $\gamma$  function is further discouraged by findings that complete loss of PKC $\gamma$  in knockout mice does not induce cerebellar degeneration (1). These clinical and experimental findings may thus fit the gain-of-function mechanism for SCA14.

Our findings suggested that oxidative stress unmasked or enhanced mutant toxicity, since cell viability was reduced by all PKC $\gamma$  mutants tested here under oxidative stress, but not by several previous mutants without stress (2). This is partly attributed to oxidative stress-induced kinase activation of



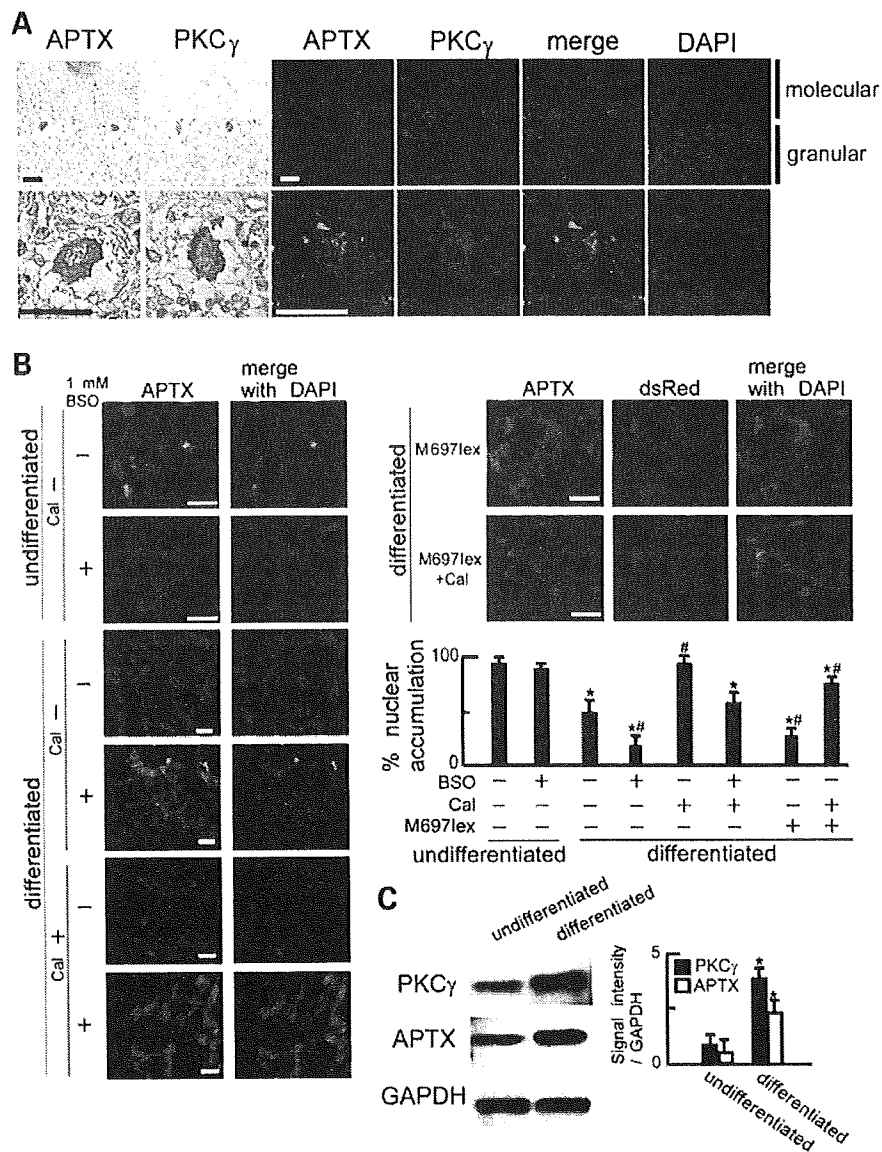


**Figure 6.** Distribution of APTX in neurons. (A) Pathological specimens of the control human cerebellum. Conventional horseradish peroxidase-based immunostaining (without nuclear counterstaining) showed that Purkinje cells had high levels of PKC $\gamma$  and APTX predominantly in the cytoplasm with small amounts of both proteins in nuclei (first and second columns). Coimmunostaining followed by confocal microscopic imaging reproduced the results (remaining columns). Scale bar represents 50  $\mu$ m. (B) Confocal microscopic analyses of PC12 cells showed that immunostained endogenous APTX was distributed in the nucleus in undifferentiated cells, but in both the cytoplasm and nucleus in differentiated cells. BSO treatment (1 mM for 12 h without cell death) as well as dsRed-M697lex expression by transfection decreased nuclear APTX in differentiated PC12 cells. Calphostin C (Cal) increased nuclear APTX. Scale bar represents 10  $\mu$ m. \* $P < 0.05$ , unpaired Student's  $t$ -test as compared with the sample for undifferentiated PC12 cells without BSO treatment. # $P < 0.05$ , unpaired Student's  $t$ -test between samples for differentiated PC12 cells as compared with the sample without BSO, Cal or M697lex. (C) Immunoblot showed that differentiation increased PKC $\gamma$  and APTX levels in PC12 cells, with a larger effect on PKC $\gamma$ . \* $P < 0.05$ , unpaired Student's  $t$ -test as compared with the sample for undifferentiated PC12 cells.

mutants. However, a few studies demonstrated that oxidative stress increased the activity of only WT (16,17). This discrepancy might be explained by different kinase assay systems employing distinct antibodies for immunoprecipitation-purification; previously used antibodies against PKC $\gamma$  inhibited kinase activities (Supplementary Material, Fig. S3), which may lead to underestimation of mutant activities. Our notion that oxidative stress increased mutant kinase activities

and cell death was further supported by the observed reduction in cell death by a specific PKC inhibitor.

#### Mutant PKC $\gamma$ phosphorylated APTX and inhibited nuclear import of APTX

Our fluorescent imaging study revealed that only APTX, a DNA repair protein responsible for autosomal recessive ataxia, was

mislocalized by mutant PKC $\gamma$  in cytoplasm. Mislocalization was confirmed with endogenous APTX. Kinase assay demonstrated that APTX is potentially an intrinsic substrate for both WT and mutant PKC $\gamma$ , but a preferential one for mutant, since the  $K_m$  values of mutants (38.2–80.6  $\mu\text{M}$ ) and WT PKC $\gamma$  (155.0  $\mu\text{M}$ ) were between those of known substrates (15–550  $\mu\text{M}$ ) with smaller  $K_m$  values for mutants (9). Fluorescent imaging and *in vitro* and *in vivo* phosphorylation studies revealed that APTX was phosphorylated and present in the cytoplasm and that the phosphorylation site was the Thr111 residue. Phosphorylation at this residue adjacent to the nuclear localization signal (residues 112–117) reduced interaction of APTX with importin  $\alpha$ , a nuclear import adaptor protein. Our recent study demonstrates that APTX is involved in the repair of oxidative-stress-induced DNA damage *in vivo* and that cell death in ataxia is caused by APTX mutations *per se* (23). Furthermore, nuclear import failure of APTX is associated with another neurological disorder, triple A syndrome (19). All these facts suggest that loss of nuclear APTX preferentially phosphorylated by mutant PKC $\gamma$  is at least partly involved in the pathomechanism of SCA14.

How mutant-PKC $\gamma$ -mediated loss of nuclear APTX leads to oxidative stress-induced cell death is critical to establishing treatment. We found that DNA damage (8-oxoG) accumulated before cell death, but was restored by increasing nuclear APTX, such as by kinase inhibitor treatment and phosphorylation-resistant APTX transfection. The involvement of DNA damage is also supported by our previous findings that reduced APTX in the nucleus or in general induced DNA damage, including 8-oxoG, before cell death in neurodegenerative diseases (19,23).

Why nervous systems, particularly cerebellar Purkinje cells, are predominantly affected in SCA14 remains unclear, partly because autopsy studies of the brains of patients with SCA14 are scant; only one case has been reported (14). Our findings in control brains and neuronal differentiated cultured cells suggest high expression levels of PKC $\gamma$  in Purkinje cells and increased PKC $\gamma$  levels during differentiation in cultured cells. Accordingly, nuclear accumulation of APTX was already reduced in these cells and further decreased by mutant PKC $\gamma$  with increased activity. In addition, neuronal cells have high requirements for ATP and are therefore exposed to high amounts of oxidative stress generated during mitochondrial oxidative phosphorylation. Such high oxidative stress produces more DNA damage than that in other cells. Collectively, we speculate that the predominant involvement of nervous systems is ascribed to PKC $\gamma$ -increase-mediated loss of nuclear APTX and oxidative stress-induced DNA damage.

Another question is whether phenotypic similarities are seen in SCA14 and APTX-related ataxia since both diseases are probably associated with loss of nuclear APTX. These diseases are characterized by progressive ataxia, cognitive impairment and involuntary movement (24), with similar brain MRI (predominant cerebellar atrophy with a preserved brainstem) and pathological findings (severe loss of cerebellar Purkinje cells). These similarities may conversely support a common neurodegenerative mechanism.

Recent studies have demonstrated that aggregate formation of mutant PKC $\gamma$  induces ER stress, leading to cell death. However, our results suggested that aggregate formation was secondary to increased kinase activity, since a kinase inhibitor

and KD-mutant PKC $\gamma$  significantly reduced aggregation (Supplementary Material, Fig. S5). In addition, ER stress blockers such as caspase 12 inhibitor z-ATAD-fmk (10–50  $\mu\text{M}$ ) and parkin did not reduce cell death in our system. Collectively, aggregation-induced ER stress may not be the primary pathomechanism of SCA14, as partly supported by a previous finding that the brain of a previous patient with SCA14 showed no PKC $\gamma$  aggregation (14).

In conclusion, our study suggests that increased kinase activity is primarily involved in the pathomechanism of SCA14. Oxidative stress further increases kinase activities and augments nuclear import failure of the DNA repair protein APTX. The resultant DNA damage, which is beyond the limited capacity of reduced APTX in the nucleus, may participate in triggering cell death. However, we cannot exclude the possibility that increased phosphorylation of other PKC $\gamma$  substrates, including MARCKS (Supplementary Material, Fig. S4), may also play a critical role in the pathomechanism of SCA14. Nevertheless, our finding that increased nuclear APTX caused by a phosphorylation-resistant form reduced oxidative stress-induced DNA damage and cell death suggests that APTX may play an essential role in the pathogenesis of SCA14. Kinase inhibitors and antioxidants may be therapeutic options for SCA14, currently an incurable disease.

## EXPERIMENTAL PROCEDURES

### Patients and genetic analyses

The proband (Patient 1), a 20-year-old woman, developed progressive cerebellar ataxia at the age of 7 years, and generalized truncal and limb myoclonus at 18 years. Detailed clinical information and real-time-PCR methods are described in the Supplementary Experimental Procedures. Her father, 49 years, and mother, 45 years, remained asymptomatic. Despite no apparent consanguinity, the grandparents lived in the same prefecture. The 86-year-old paternal grandmother (Patient 2) had progressive ataxia without myoclonus, starting at 60 years. The maternal grandmother, whose medical records were not available, had late-onset parkinsonism and died at 78 years. After obtaining written informed consent, genetic testing was performed using lymphocytes of Patients 1 and 2. The parents declined testing. Abnormal triplet repeat expansions in the genes for SCA 1, 2, 3, 6, 7, 8, 12 and 17, and DRPLA were negative. PCR-direct sequencing showed no mutations in the APTX gene (25). The *PRKCG* gene was sequenced as described previously (24). The *PRKCG* gene and cDNA in lymphocytes were quantified by real-time-PCR methods.

### Vector construction, cell culture and transfection

N-terminal GFP-parkin and WT (Q30) ataxin1 plasmids were generated from the cloned cDNAs kindly donated by Drs Hattori and Zoghbi. Plasmid vectors expressing C-terminal-GFP-WT-PKC $\gamma$ , and N-terminal GFP-XPA, ATM, CAF-1, SMN1 and DNA ligase I were generously donated by Drs Howell, Vermeulen, Khanna, Yasui, Matra and Leonhardt, respectively (26). Detailed information on other plasmids used and on cell culture is described in the Supplementary Experimental Procedures.

### Immunoblot analyses

Whole cell lysates from SH-SY5Y cells 24 h after transfection with cDNAs encoding untagged or GFP-PKC $\gamma$  proteins were immunoblotted with antibodies to PKC $\gamma$  (Invitrogen Corp., Carlsbad, CA, USA), GFP, or actin antibodies (Santa Cruz Biotech., Inc., Santa Cruz, CA, USA). Expression levels of mRNA encoding GFP- and untagged PKC $\gamma$  were quantified by real-time-RT-PCR after DNase treatment to eliminate plasmid DNA contamination. Whole cell lysates from PC12 cells were subjected to western blot with anti-PKC $\gamma$ , anti-APT $\gamma$  and anti-GAPDH antibodies. Phosphorylation of MARCKS was assessed by immunoblotting with anti-MARCKS (Santa Cruz Biotech., Inc.) and anti-phosphorylated MARCKS (Chemicon, Millipore Corp., Temecula, CA, USA) antibodies, using SH-SY5Y cells expressing WT, S119F, or M697Iex-GFP-PKC $\gamma$  proteins for 24 h after transfection, with or without 1 mM BSO treatment for 12 h. Relative amounts of proteins were calculated with the use of a chemiluminescence-based method and an LAS-1000 lumino-image analyzer (Fuji Film, Tokyo, Japan).

### Kinase assay of PKC $\gamma$

Various GFP-PKC $\gamma$  proteins 24 h after transfection to SH-SY5Y cells with or without 1 mM BSO treatment for 12 h were immunoprecipitated with anti-GFP-antibody and subjected to kinase assay, using a peptide substrate-based PKC assay kit (Upstate, Millipore Corp.) (5). Phosphorylation of full-length human APTX was measured using WT and mutant (T111A and S118A) APTX, synthesized in *Escherichia coli*, purified by GST column, and cleaved by Precision protease (GE Healthcare) to remove GST (21,27). Km and kcat values were calculated with the Michaelis–Menten equation. The following peptides around Thr111 were generated and used as substrates: WT, KNPGLE7HRKRKR and T111A, KNPGLE4HRKRKR (Medical & Biological Laboratories Co., Ltd, Nagoya, Japan). Phosphorylated APTX proteins and peptides were then electrophoresed on 5–20 and 20% polyacrylamide gels, respectively, dried, and exposed to X-ray films. To examine dominant negative effects, kinase activities of WT coexpressed with mutant GFP-PKC $\gamma$  were compared with those coexpressed with GFP. Inhibitory activities of the anti-PKC $\gamma$  antibody (BD Biosciences., San Jose, CA, USA) previously used for kinase assay (6) were measured by adding various concentrations of the antibody to our assay solution.

### In vivo phosphorylation

Phosphorylation of APTX in cells was performed essentially according to the previous method (28). SH-SY5Y cells,  $2 \times 10^6$ , were seeded on 100-mm plates. WT, S119F and M697Iex-dsRed-PKC $\gamma$  plasmids were separately cotransfected with WT or T111A-GFP-APT $\gamma$  to the cells and incubated for 24 h with or without 6 h-treatment with calphostin C. Cells were washed twice with phosphate-free DMEM (Invitrogen, #11971025) and then incubated for 3 h in the same medium containing 10% dialyzed fetal bovine serum and 300  $\mu$ Ci [ $^{32}$ P]orthophosphate (Amersham Pharmacia Biothech).

Cells were washed with PBS and lysed with buffers in NE-PER kit to separate nuclear and cytoplasmic fractions (Thermo Fisher Scientific Inc., Rockford, IL, USA). Lysates were subjected to immunoprecipitation with anti-GFP antibody. Purified GFP-APT $\gamma$  was electrophoresed, dried and exposed to X-ray films. The same samples were immunoblotted with anti-APT $\gamma$  antibody. In this assay condition (>10 min exposure), signals of chemiluminescence from immunoprecipitated APT $\gamma$  were much stronger than those of labeled radioisotope, which might affect the immunoblotting results. Separated lysates before immunoprecipitation (input) were also immunoblotted with antibodies against APT $\gamma$ , histone H3 (a nuclear marker), and GAPDH (a cytoplasmic marker) to ensure successful subcellular fractionation.

### BSO-susceptibility and rescue of cells expressing mutant PKC $\gamma$

Cells transfected separately with WT and mutant PKC $\gamma$  plasmids were treated with 0–1 mM BSO for 24 h and subjected to MTS assay. Cell viability was confirmed by propidium iodide exclusion assay. Correlations between cell death ratios and kinase activities under oxidative stress were assessed by linear regression analyses. Dosage effects of M697Iex and S119F were assessed by transfection with 0–4  $\mu$ g cDNA. Total plasmid DNA amounts were adjusted using additional GFP vector (0–3  $\mu$ g) to maintain a constant transfection efficiency.

Nuclear accumulation of APT $\gamma$ , 8-oxoG immunoreactivity, and cell viability in SH-SY5Y cells expressing S119F mutant PKC $\gamma$  in the presence of 1 mM BSO were observed after the following treatments: the selective PKC inhibitor calphostin C (SIGMA) for 6 h, and the caspase 12 inhibitor z-ATAD-fmk (BioVision, Inc., Mountain View, CA, USA), DEC (SIGMA), and all-*trans*-retinol (SIGMA) for 24 h. Similar variables were measured on cotransfection with WT/mutant APT $\gamma$  and parkin. For control, SH-SY5Y cells were transfected with APT $\gamma$  si576 plasmid and treated with 1 mM BSO.

### Fluorescent imaging

Detailed methods are described in the Supplemental Experimental Procedures. Briefly, live SH-SY5Y cells 24 h after transfection with plasmids encoding dsRed-APT $\gamma$  and/or untagged PKC $\gamma$  and treated with 0–1 mM BSO for 10 h were quantitatively observed using a fluorescent microscope. For 8-oxoG immunostaining, cells were fixed in 4% paraformaldehyde. The cerebellum of controls, who had died of myocardial infarction, was immunostained with APT $\gamma$  and PKC $\gamma$ . PC12 cells were treated with or without BSO. Differentiated cells were further treated with or without calphostin C. After fixation, immunostained endogenous APT $\gamma$  was visualized using a confocal microscope.

### Immunoprecipitation of APTX and PKC $\gamma$ /importin $\alpha$

GFP-PKC $\gamma$  expressed in SH-SY5Y cells was immunoprecipitated with anti-GFP antibody, and immunoblotted with anti-GFP antibody and monoclonal anti-APT $\gamma$  antibody to detect endogenous APT $\gamma$ . Immunoprecipitation of endogenous APT $\gamma$  with the monoclonal antibody and subsequent

immunoblotting with anti-GFP antibody and rabbit polyclonal anti-APT $\alpha$  antibody (Bethyl Laboratories, Inc., Montgomery, TX, USA) was conversely performed.

Unphosphorylated and/or phosphorylated dsRed-APT $\alpha$  expressed in SH-SY5Y cells was immunoprecipitated with anti-APT $\alpha$  monoclonal antibody and subjected to western blot with antibodies to APT $\alpha$  and endogenous importin  $\alpha$ . Conversely, endogenous importin  $\alpha$  was immunoprecipitated, and APT $\alpha$  and importin  $\alpha$  were detected by western blot.

## ACKNOWLEDGEMENTS

The authors thank Drs Howell (NINDS/NIH), Matera (Case Western Reserve University, Cleveland, OH, USA), Vermeulen (Center for Biomedical Genetics, Medical Genetic Center, Netherlands), Khanna (Signal Transduction Laboratory, Queensland Institute of Medical Research, Brisbane, Australia), Yasui (Tohoku University, Sendai, Japan), Leonhardt (Ludwig Maximilians University, Germany), Hattori (Juntendo University, Tokyo, Japan) and Zoghbi (Baylor College of Medicine, TX, USA) for the gifts of plasmid vectors.

*Conflict of Interest statement.* None declared.

## FUNDING

This study was partly supported by Health and Labour Sciences Research Grants (Research in intractable diseases) and Grants-in-Aids for Scientific Research from the Ministry of Education, Culture, Sports, Science and Technology of Japan (to Drs Hirano and Ueno).

## REFERENCES

- Chen, C., Kano, M., Abeliovich, A., Chen, L., Bao, S., Kim, J.J., Hashimoto, K., Thompson, R.F. and Tonegawa, S. (1995) Impaired motor coordination correlates with persistent multiple climbing fiber innervation in PKC gamma mutant mice. *Cell*, **83**, 1233–1242.
- Seki, T., Adachi, N., Ono, Y., Mochizuki, H., Hiramoto, K., Amano, T., Matsubayashi, H., Matsumoto, M., Kawakami, H., Saito, N. *et al.* (2005) Mutant protein kinase C gamma found in spinocerebellar ataxia type 14 is susceptible to aggregation and causes cell death. *J. Biol. Chem.*, **280**, 29096–29106.
- Chen, D.H., Cimino, P.J., Ranum, L.P., Zoghbi, H.Y., Yabe, I., Schut, L., Margolis, R.L., Lipe, H.P., Feleke, A., Matsushita, M. *et al.* (2005) The clinical and genetic spectrum of spinocerebellar ataxia 14. *Neurology*, **64**, 1258–1260.
- Doran, G., Davies, K.E. and Talbot, K. (2008) Activation of mutant protein kinase C gamma leads to aberrant sequestration and impairment of its cellular function. *Biochem. Biophys. Res. Commun.*, **372**, 447–453.
- Verbeek, D.S., Knight, M.A., Harmison, G.G., Fischbeck, K.H. and Howell, B.W. (2005) Protein kinase C gamma mutations in spinocerebellar ataxia 14 increase kinase activity and alter membrane targeting. *Brain*, **128**, 436–442.
- Zhang, Y., Snider, A., Willard, L., Takemoto, D.J. and Lin, D. (2009) Loss of Purkinje cells in the PKC gamma H101Y transgenic mouse. *Biochem. Biophys. Res. Commun.*, **378**, 524–528.
- Seki, T., Takahashi, H., Adachi, N., Abc, N., Shimahara, T., Saito, N. and Sakai, N. (2007) Aggregate formation of mutant protein kinase C gamma found in spinocerebellar ataxia type 14 impairs ubiquitin-proteasome system and induces endoplasmic reticulum stress. *Eur. J. Neurosci.*, **26**, 3126–3140.
- Lim, J., Hao, T., Shaw, C., Patel, A.J., Szabo, G., Rual, J.F., Fisk, C.J., Li, N., Smolyar, A., Hill, D.E. *et al.* (2006) A protein-protein interaction network for human inherited ataxias and disorders of Purkinje cell degeneration. *Cell*, **125**, 801–814.
- Marais, R.M., Nguyen, O., Woodgett, J.R. and Parker, P.J. (1990) Studies on the primary sequence requirements for PKC-alpha, -beta 1 and -gamma peptide substrates. *FEBS Lett.*, **277**, 151–155.
- Xiao, D.M., Pak, J.H., Wang, X., Sato, T., Huang, F.L., Chen, H.C. and Huang, K.P. (2000) Phosphorylation of HMG-I by protein kinase C attenuates its binding affinity to the promoter regions of protein kinase C gamma and neurogranin/RC3 genes. *J. Neurochem.*, **74**, 392–399.
- Ramakers, G.M., Gerendasy, D.D. and de Graan, P.N. (1999) Substrate phosphorylation in the protein kinase C gamma knockout mouse. *J. Biol. Chem.*, **274**, 1873–1874.
- Kim, C.H., Braud, S., Isaac, J.T. and Roche, K.W. (2005) Protein kinase C phosphorylation of the metabotropic glutamate receptor mGluR5 on Serine 839 regulates Ca<sup>2+</sup> oscillations. *J. Biol. Chem.*, **280**, 25409–25415.
- Williams, R. and Coluccio, L.M. (1995) Phosphorylation of myosin-I from rat liver by protein kinase C reduces calmodulin binding. *Biochem. Biophys. Res. Commun.*, **216**, 90–102.
- Chen, D.H., Brkanac, Z., Verlinde, C.L., Tan, X.J., Bylenok, L., Noehlin, D., Matsushita, M., Lipe, H., Wolff, J., Fernandez, M. *et al.* (2003) Missense mutations in the regulatory domain of PKC gamma: a new mechanism for dominant nonepisodic cerebellar ataxia. *Am. J. Hum. Genet.*, **72**, 839–849.
- Adachi, N., Kobayashi, T., Takahashi, H., Kawasaki, T., Shirai, Y., Ueyama, T., Matsuda, T., Seki, T., Sakai, N. and Saito, N. (2008) Enzymological analysis of mutant protein kinase C gamma causing spinocerebellar ataxia type 14 and dysfunction in Ca<sup>2+</sup> homeostasis. *J. Biol. Chem.*, **283**, 19854–19863.
- Lin, D. and Takemoto, D.J. (2005) Oxidative activation of protein kinase C gamma through the C1 domain. Effects on gap junctions. *J. Biol. Chem.*, **280**, 13682–13693.
- Lin, D. and Takemoto, D.J. (2007) Protection from ataxia-linked apoptosis by gap junction inhibitors. *Biochem. Biophys. Res. Commun.*, **362**, 982–987.
- Verbeek, D.S., Goedhart, J., Bruinsma, L., Sinke, R.J. and Reits, E.A. (2008) PKC gamma mutations in spinocerebellar ataxia type 14 affect C1 domain accessibility and kinase activity leading to aberrant MAPK signaling. *J. Cell Sci.*, **121**, 2339–2349.
- Hirano, M., Furiya, Y., Asai, H., Yasui, A. and Ueno, S. (2006) ALADINI482S causes selective failure of nuclear protein import and hypersensitivity to oxidative stress in triple A syndrome. *Proc. Natl. Acad. Sci. USA*, **103**, 2298–2303.
- Kuwahara, H., Nishizaki, M. and Kanazawa, H. (2008) Nuclear localization signal and phosphorylation of Serine350 specify intracellular localization of DRAK2. *J. Biochem.*, **143**, 349–358.
- Hirano, M., Furiya, Y., Kariya, S., Nishiwaki, T. and Ueno, S. (2004) Loss of function mechanism in aprataxin-related early-onset ataxia. *Biochem. Biophys. Res. Commun.*, **322**, 380–386.
- Shimohama, S., Saitoh, T. and Gage, F.H. (1990) Differential expression of protein kinase C isozymes in rat cerebellum. *J. Chem. Neuroanat.*, **3**, 367–375.
- Hirano, M., Yamamoto, A., Mori, T., Lan, L., Iwamoto, T.A., Aoki, M., Shimada, K., Furiya, Y., Kariya, S., Asai, H. *et al.* (2007) DNA single-strand break repair is impaired in aprataxin-related ataxia. *Ann. Neurol.*, **61**, 162–174.
- Klebe, S., Durr, A., Rentschler, A., Hahn-Barma, V., Abele, M., Bouslam, N., Schols, L., Jedynak, P., Forlani, S., Denis, E. *et al.* (2005) New mutations in protein kinase C gamma associated with spinocerebellar ataxia type 14. *Ann. Neurol.*, **58**, 720–729.
- Hirano, M., Nishiwaki, T., Kariya, S., Furiya, Y., Kawahara, M. and Ueno, S. (2004) Novel splice variants increase molecular diversity of aprataxin, the gene responsible for early-onset ataxia with ocular motor apraxia and hypoalbuminemia. *Neurosci. Lett.*, **366**, 120–125.
- Kiryama, T., Hirano, M., Asai, H., Ikeda, M., Furiya, Y. and Ueno, S. (2008) Restoration of nuclear-import failure caused by triple A syndrome and oxidative stress. *Biochem. Biophys. Res. Commun.*, **374**, 631–634.
- Hirano, M., Asai, H., Kiriyama, T., Furiya, Y., Iwamoto, T., Nishiwaki, T., Yamamoto, A., Mori, T. and Ueno, S. (2007) Short half-lives of ataxia-associated aprataxin proteins in neuronal cells. *Neurosci. Lett.*, **419**, 184–187.
- Even-Faitelson, L. and Ravid, S. (2006) PAK1 and aPKCzeta regulate myosin II-B phosphorylation: a novel signaling pathway regulating filament assembly. *Mol. Biol. Cell*, **17**, 2869–2881.

〈総説〉

## 神経疾患と塩基除去修復

奈良県立医科大学 1 神経内科、2 ラジオアイソトープ実験施設  
平野牧人\*<sup>1</sup>、森 俊雄<sup>2</sup>、上野 聡<sup>1</sup>

### はじめに

塩基除去修復 (base excision repair: BER) の対象となるDNA損傷は、主として活性酸素により生じる。活性酸素によるDNA損傷は哺乳類の細胞1個あたり1日50,000~100,000個生じるとされ(1)、代表的な損傷塩基である8-オキシグアニンは細胞によって異なるが、10<sup>6</sup>塩基あたり常に0.07~145個存在しているとされる(2)。この活性酸素が発生する負荷を酸化ストレスと呼び、DNAのみならず、脂質、蛋白を障害する。酸化ストレスは病的状態のみを指すのではなく、生理的条件下であっても、酸素を消費して酸化的リン酸化によりATPを産生する際には、過酸化水素さらにヒドロキシラジカルといった活性酸素を生じるため、細胞は常に酸化ストレスにさらされていると言える。正常では、こうして生じたDNA損傷は転写・翻訳障害が起きないようにBERによって取り除かれる。

神経細胞は酸化ストレスに感受性が高いとされる。なぜなら、酸素消費が他臓器の10倍近くあり、そのため多量の活性酸素が発生するからである。他の理由としては、障害された細胞を取り除き、正常細胞を分裂して代替するといった修復が行えない事、さらに分裂時に利用できる正確性の高い相同組換えによるDNA修復が行えない事が挙げられる。修復蛋白に異常がある場合、あるいは酸化ストレスが許容量を超えた時、神経細胞の機能低下さらに細胞死、すなわち神経変性が生じると考えられる。ここでは、私たちの最近の研究を含め、BERに関連する神経変性疾患であるパーキンソン病、脊髄小脳変性症、運動ニューロン病 (筋萎縮側索硬化症、AAA症候群) を紹介する。

### 1. パーキンソン病

パーキンソン病は無動 (運動減少)、固縮 (筋緊張亢進)、振戦 (手足の震え) を特徴とする、主として50歳以降に発症する神経変性疾患であり、本邦においては、人口10万人あたり約120人

---

\*〒634-8522 奈良県橿原市四条町840

TEL:0744-22-3051 FAX:0744-24-6065 e-mail:hirano\_makito@yahoo.co.jp

キーワード：神経変性疾患、DNA修復、酸化ストレス

が罹患しているとされる(3,4)。アメリカでは、映画バック・トゥ・ザ・フューチャーの主人公を演じたマイケル・J・フォックスや、ボクシング元世界チャンピオンのモハメド・アリが罹患した事で有名である。大部分は原因不明(弧発例)であるが、一部には遺伝性のものが知られる。原因遺伝子は、 $\alpha$ -synuclein, parkin, DJ-1, PINK1, UCHL1, LRRK2, HtrA2/Omi, ATP13A2が同定され、さらに最近GIGYF2, FBXO7, PLA2G6などがまだ症例が少ないながら原因遺伝子として報告された(5-7)。典型的パーキンソン病の病理像は、中脳にある黒質ドーパミン分泌細胞の変性である。BERとの関連では、弧発例の尿に8-ヒドロキシデオキシグアノシン(8-オキソグアノシンの分解産物)が増加することが知られる(8)。また、弧発例の脳に8-オキソグアノシンの修復酵素であるOGG1が増加している事が報告されている(9)。ごく最近、常染色体劣性パーキンソン病の原因となるParkin遺伝子のノックアウトマウス脳において、神経細胞に8-オキソグアノシンが顕著に蓄積していることが報告された(10)。ParkinはE3ユビキチンリガーゼであり、本来細胞質とくにER・ゴルジ体に存在する蛋白と考えられているが、核内にある修復の足場蛋白PCNAと結合、活性を促進していると報告された。しかし、その促進の機序については不明である。PCNAを直接ユビキチン化しないとされている。パーキンの基質として、これまで、10を超える蛋白が同定されている。主なものとして、CDCrel-1, Pael-receptor, synphilin-1, cyclin E,  $\alpha/\beta$ -tubulin, p38 subunit of aminoacyl-tRNA-transferase, poly-glutamine protein, RanBP2, PDCD2-1などが挙げられる(11,12)。なお、初期には常染色体優性遺伝パーキンソン病の原因遺伝子 $\alpha$ -シヌクレインの糖化物質も基質とされたが、追試されていない。パーキンの機能喪失により、こういった基質がユビキチン化されないため、プロテアゾーム分解されずに蓄積するが、このうちどれが神経変性に直接関与するかは、結論がでていない。未同定の基質が関与しているかもしれない。

なぜ、弧発性・遺伝性パーキンソン病でBERの基質である8-オキソグアノシンが増加しているかの詳細は不明であるが、中脳のドーパミン分泌細胞は神経メラニンを含み、鉄含有率も高いため、活性酸素の発生が多く、DNA損傷発生も多いと考えられる。あるいは、パーキンソン病の発生を促進する因子に農薬、殺虫剤などへの暴露が挙げられるが、そういった薬剤がDNA損傷を増加させることも、一因かもしれない。現在のところDNA損傷が、本疾患における細胞障害の主因であるかは不明であるが、他疾患の研究から、少なくともその一端を担うと考えられる。

本疾患の根治療法はないが、症状を抑えるために使用される薬剤として、ドーパミンの原料となるレボドパ製剤、ドーパミンの分解阻害薬、ドーパミン受容体刺激薬、ドーパミン放出促進薬などが知られている。このうち、細胞培養ではレボドパに酸化ストレス増加作用や細胞毒性があり、一方ドーパミン受容体刺激薬には細胞保護作用が報告されている。ただし、患者尿中の8-オキソグアノシン濃度はレボドパに必ずしも一致しなかった(8)。現在、副作用の少なく、細胞保護作用を有する薬剤の開発が盛んに行なわれている。



## 2. 脊髄小脳変性症

脊髄小脳変性症は脊髄や小脳を障害する、様々な弧発性・遺伝性疾患の総称である。全体として人口10万人あたり5-10人が罹患している。代表的な疾患としては、常染色体優性遺伝の遺伝性小脳失調症1型 (SCA1)、ジョセフ病 (SCA3)、歯状核赤核淡蒼球ルイ体萎縮症 (DRPLA) などのポリグルタミン病が含まれる。これらのポリグルタミン病も病態機序の一部に、DNA修復の関与が報告されているが、それはBERではなくヌクレオチド除去修復やDNA二本鎖切断修復である(12,13)。一方、BER/DNA単鎖切断修復に直接関連する疾患として、2001年本邦の辻らとフランスのKoenigらにより原因遺伝子アラタキシンが同定された眼球運動失行と低アルブミン血症を伴う早発型脊髄小脳失調症 (Early-onset ataxia with ocular motor apraxia and hypoalbuminemia [EAOH]/ataxia oculomotor apraxia [AOA1]) が認知されるようになった(14,15)。特殊な病気のように見えるが、ヨーロッパではアラタキシン異常のあるフリートライヒ失調症に次いで多い常染色体劣性小脳失調症である。本邦では、最も多い常染色体劣性小脳失調症であり、驚いた事にこれまでフリートライヒ失調症と言われていた多くが、EAOHである事が判明した。逆にアラタキシン遺伝子異常は未だ発見されていない。症状は両者で類似しており、進行性の小脳失調 (体のふらつきとなめらかな手足の動きができなくなる) と末梢神経障害 (感覚の低下、手足の筋肉が痩せる) が見られる。しかし、EAOHではそれらに加え、意識的に眼球を動かすことが困難になる眼球運動失行や、低アルブミン血症がみられる。病理像やMRI画像も両者では異なり、フリートライヒ失調症では小脳が保たれるのに対し、EAOHでは小脳の顕著な萎縮が見られる (図1)。低アルブミン血症の原因は肝臓でのアルブミン合成低下とされるが、その詳細は不明である。私たちが最近行なった研究で、EAOHは変異アラタキシンの活性低下または蛋白の不安定化による機能喪失によって生じ、その結果DNA修復障害をきたすことが判明した(16-18)。また、小脳の病理像では、大型細胞であるPurkinje細胞の脱落が認められ、顆粒神経も減少し、

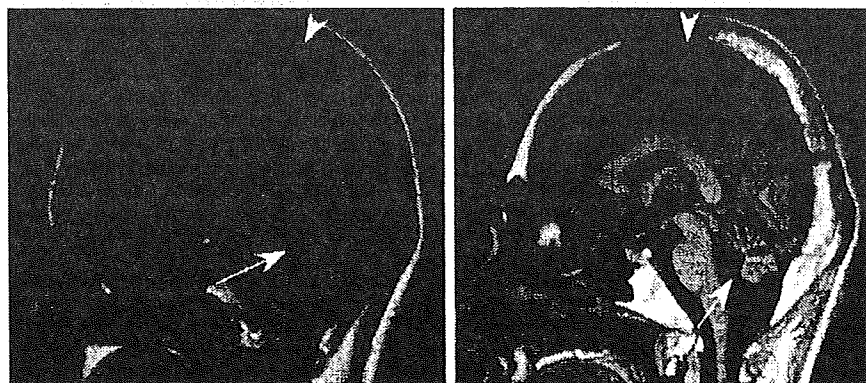


図1. MRI矢状断T1強調画像。対照(左)に比してEAOH患者(右)の小脳(矢印)は著明に萎縮している。一方、大脳(矢頭)は保たれている。

間質が増加する(図2)。残された顆粒神経の核に8-オキシグアニンの染色性が増加していた(18)。

原因遺伝子アプラタキシンは単鎖切断修復に関与すると考えられ、BERの過程あるいは活性酸素の直接効果により生じる単鎖切断の末端処理を行なうとされる。5'端に生じるAMP化(19)あるいは3'端のリン酸基を除去する活性を有する(20)。これらの作用とBERへの影響であるが、単鎖切断修復遅延により単鎖切断が残った状態では、近傍の塩基損傷に対して、二本鎖切断を避けるために、BERが遅延し、8-オキシグアニンなどの損傷塩基が増加すると考えられる(21)。

現在EAOHの根治療法はないが、抗酸化剤により損傷塩基や単鎖切断を減らす事で、低下した修復能力を補い、細胞障害を抑制する事が、培養細胞レベルでは認められる(18)。

### 3. 筋萎縮性側索硬化症

本疾患は、進行性の筋萎縮、筋力低下を主徴とし、主として50歳以降に発症する神経変性疾患であり、本邦では人口10万人あたり約5人が罹患している(22)。アメリカでは大リーグのニューヨーク・ヤンキースに属していたルー・ゲーリックが罹患した事から、ルー・ゲーリック病とも言われる。他の神経変性疾患に比べ進行が早く、診断から約3年で呼吸障害や感染症で死亡する。また、いわゆる寝たきりの被介護者となる最も多い疾患の一つであり、医学的・社会的に大きな

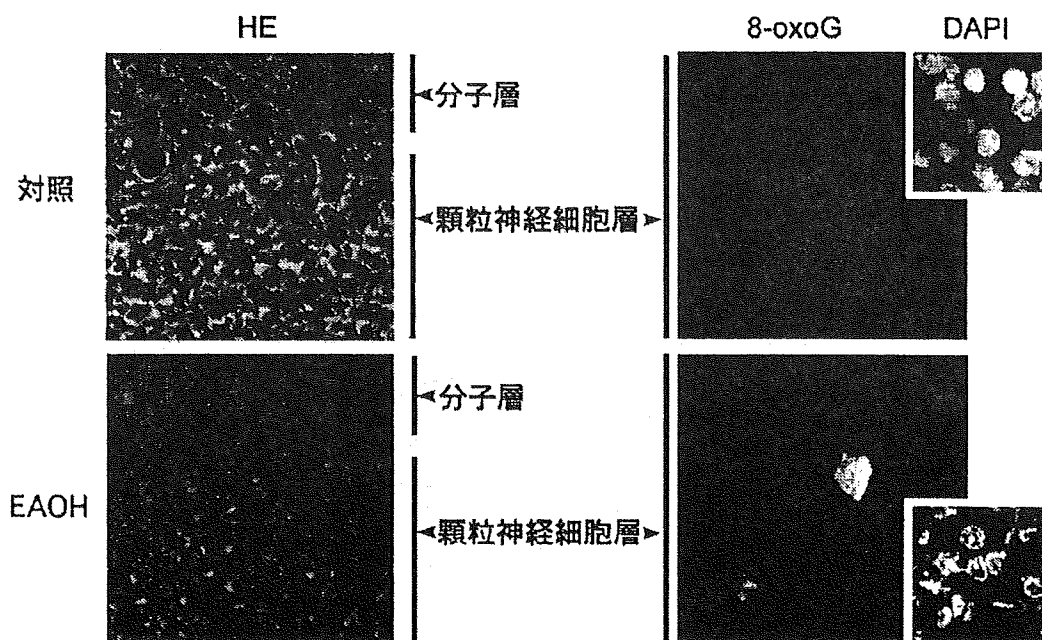


図2. 小脳皮質病理像。ヘマトキシリン・エオジン(HE)染色標本において、対照では分子層と顆粒神経細胞層の間にPurkinje細胞(矢印)が存在するが、EAOH患者では消失している。また、顆粒神経の核も患者では減少しており、間質が増加している。8-オキシグアニン(8-oxoG)の免疫染色(強拡大)では、患者の顆粒神経の核のみ染色性が亢進している。DAPIは同部の核染色を示す。

問題となっている。大部分は原因不明（孤発例）であるが、約10%に遺伝性のものが知られる。原因遺伝子には、Cu, Zn superoxide dismutase (SOD1), ALSIN (ALS2), SETX (senataxin), TDP43, ANG, VAPB, seipin (BCL2), VCPなどが知られる(23)。病理像は大脳皮質にある上位運動ニューロンおよび脊髄前核や脳幹にある下位運動ニューロンの変性・脱落である。BERとの関連では、患者脳・脊髄に8-オキシグアニンの上昇および、BERを担うAPEの上昇が認められる(24,25)。また、遺伝性筋萎縮性側索硬化症の原因となるSOD1のトランスジェニック動物モデルでは、運動ニューロンの核内SOD1が減少し、さらに細胞モデルで単鎖切断の増加する事も報告された(26)。核内の活性酸素除去に働くSOD1の減少が、DNA損傷を増加させると推定されている。

現在、根治療法はないが、患者への活性酸素除去剤エダラボン点滴静注の大規模臨床試験が本邦で始まっており、その結果が待たれる(27)。

#### 4. AAA症候群

AAA(トリプルA)症候群は食道アカラシア(Achalasia: 飲み込みにくい)、無涙症(Alacrima)、副腎皮質機能不全(Adrenal insufficiency: 血糖値の低下など)の3徴候に筋萎縮、筋力低下が合併する常染色体劣性疾患である。原因遺伝子アラジンが同定されているが遺伝子異常が検出されない原因不明例が1/3以上を占める。まれな疾患であり、全世界で遺伝子異常のある例が約150例、本邦ではわずか、6例が報告されるのみである。しかし、発症年齢が0-35歳と幅広く、症状の重症度も様々であるため、正確な診断は比較的困難であり、症例数は報告よりも多いと考えられる。実際、私たちの1症例では他院で13年間診療されていたが、診断に至らなかった。神経難病である筋萎縮性側索硬化症と共通する神経徴候(上位・下位運動ニューロン障害)を呈するが、10年以上にわたる緩徐な進行を示す。AAA症候群の原因蛋白アラジンは、細胞質-核間輸送を担う核膜孔を形成する。私たちの最近の研究で、患者線維芽細胞を用いて、病態機序の一端を明らかにした。すなわち、患者細胞では小脳失調原因蛋白アプラタキシンおよびDNAリガーゼIの核内輸送が障害されており、酸化ストレスによるDNA損傷の修復が困難となり、細胞死に至る。抗酸化剤は細胞死を抑制した(28)。本細胞でも、酸化ストレスを負荷すると、核内に8-オキシグアニンが蓄積する。また、核内にアプラタキシンやDNAリガーゼIを強制的に発現させると、細胞死は軽減する(28,29)。

#### おわりに

神経細胞のうち、大型のPurkinje細胞や運動ニューロン、あるいは神経メラニンに富む黒質のドーパミン分泌細胞は特に酸化ストレスに伴うDNA損傷に脆弱であるように考えられる。代謝が非常に活発でありATP消費が多いことや、生化学的に、活性酸素産生が多い事が原因と考え

られる。こういった細胞に対して、抗酸化剤は疾患治療に応用できるように思われる。また、病態機序に基づく治療 (mechanism-based-therapy) のためにも、DNA損傷修復とくにBERのどの修復段階・蛋白が関与しているかを分子レベルで明らかにする事も今後の課題である。

## 謝辞

本研究の一部は文部科学省科学研究費補助金と厚生労働科学研究費補助金 (難治性疾患克服研究事業) によって行なわれました。共同研究をして下さった、東北大学加齢医学研究所 安井明先生、同 神経内科 糸山泰人先生、青木正志先生、奈良県立医科大学病理病態学、小西 登先生、島田啓司先生に深謝します。

## 参考文献

1. Brosh, R. M., Jr. and Bohr, V. A. Human premature aging, DNA repair and RecQ helicases. *Nucleic Acids Res*, 35: 7527-7544, 2007.
2. De Bont, R. and van Larebeke, N. Endogenous DNA damage in humans: a review of quantitative data. *Mutagenesis*, 19: 169-185, 2004.
3. 斎藤能彦、長谷川正俊、細井裕司他。医療の最先端—奈良医大からの発信—、創元社、大阪、P44-P48, 2008
4. 杉本敏夫、東野義之、南 武志他。ケアマネジメント用語辞典 ミネルバ書房、京都、P415-P416, 2007
5. Kitada, T., Asakawa, S., Hattori, N., Matsumine, H., Yamamura, Y., Minoshima, S., Yokochi, M., Mizuno, Y., and Shimizu, N. Mutations in the parkin gene cause autosomal recessive juvenile parkinsonism. *Nature*, 392: 605-608, 1998.
6. Mizuno, Y., Hattori, N., Yoshino, H., Hatano, Y., Satoh, K., Tomiyama, H., and Li, Y. Progress in familial Parkinson's disease. *J Neural Transm Suppl* 191-204, 2006.
7. Lesage, S. and Brice, A. Parkinson's disease: from monogenic forms to genetic susceptibility factors. *Hum Mol Genet*, 18: R48-59, 2009.
8. Sato, S., Mizuno, Y., and Hattori, N. Urinary 8-hydroxydeoxyguanosine levels as a biomarker for progression of Parkinson disease. *Neurology*, 64: 1081-1083, 2005.
9. Fukae, J., Takanashi, M., Kubo, S., Nishioka, K., Nakabeppu, Y., Mori, H., Mizuno, Y., and Hattori, N. Expression of 8-oxoguanine DNA glycosylase (OGG1) in Parkinson's disease and related neurodegenerative disorders. *Acta Neuropathol*, 109: 256-262, 2005.
10. Kao, S. Y. Regulation of DNA repair by parkin. *Biochem Biophys Res Commun*, 382: 321-325, 2009.
11. Fukae, J., Sato, S., Shiba, K., Sato, K., Mori, H., Sharp, P. A., Mizuno, Y., and Hattori, N. Programmed cell death-2 isoform1 is ubiquitinated by parkin and increased in the substantia nigra of patients with autosomal recessive Parkinson's disease. *FEBS Lett*, 583: 521-525, 2009.
12. Wang, G., Sawai, N., Kotliarova, S., Kanazawa, I., and Nukina, N. Ataxin-3, the MJD1 gene product, interacts with the two human homologs of yeast DNA repair protein RAD23, HHR23A and HHR23B. *Hum Mol Genet*, 9: 1795-1803, 2000.
13. Giuliano, P., De Cristofaro, T., Affaitati, A., Pizzulo, G. M., Feliciello, A., Criscuolo, C., De Michele, G., Filla, A., Avvedimento, E. V., and Varrone, S. DNA damage induced by polyglutamine-expanded proteins. *Hum Mol Genet*, 12: 2301-2309, 2003.

14. Date, H., Onodera, O., Tanaka, H., Iwabuchi, K., Uekawa, K., Igarashi, S., Koike, R., Hiroi, T., Yuasa, T., Awaya, Y., Sakai, T., Takahashi, T., Nagatomo, H., Sekijima, Y., Kawachi, I., Takiyama, Y., Nishizawa, M., Fukuhara, N., Saito, K., Sugano, S., and Tsuji, S. Early-onset ataxia with ocular motor apraxia and hypoalbuminemia is caused by mutations in a new HIT superfamily gene. *Nat Genet*, 29: 184-188, 2001.
15. Moreira, M. C., Barbot, C., Tachi, N., Kozuka, N., Uchida, E., Gibson, T., Mendonca, P., Costa, M., Barros, J., Yanagisawa, T., Watanabe, M., Ikeda, Y., Aoki, M., Nagata, T., Coutinho, P., Sequeiros, J., and Koenig, M. The gene mutated in ataxia-ocular apraxia 1 encodes the new HIT/Zn-finger protein aprataxin. *Nat Genet*, 29: 189-193, 2001.
16. Hirano, M., Furiya, Y., Kariya, S., Nishiwaki, T., and Ueno, S. Loss of function mechanism in aprataxin-related early-onset ataxia. *Biochem Biophys Res Commun*, 322: 380-386, 2004.
17. Hirano, M., Asai, H., Kiriya, T., Furiya, Y., Iwamoto, T., Nishiwaki, T., Yamamoto, A., Mori, T., and Ueno, S. Short half-lives of ataxia-associated aprataxin proteins in neuronal cells. *Neurosci Lett*, 419: 184-187, 2007.
18. Hirano, M., Yamamoto, A., Mori, T., Lan, L., Iwamoto, T. A., Aoki, M., Shimada, K., Furiya, Y., Kariya, S., Asai, H., Yasui, A., Nishiwaki, T., Imoto, K., Kobayashi, N., Kiriya, T., Nagata, T., Konishi, N., Itoyama, Y., and Ueno, S. DNA single-strand break repair is impaired in aprataxin-related ataxia. *Ann Neurol*, 61: 162-174, 2007.
19. Ahel, I., Rass, U., El-Khamisy, S. F., Katyal, S., Clements, P. M., McKinnon, P. J., Caldecott, K. W., and West, S. C. The neurodegenerative disease protein aprataxin resolves abortive DNA ligation intermediates. *Nature*, 443: 713-716, 2006.
20. Takahashi, T., Tada, M., Igarashi, S., Koyama, A., Date, H., Yokoseki, A., Shiga, A., Yoshida, Y., Tsuji, S., Nishizawa, M., and Onodera, O. Aprataxin, causative gene product for EAOH/AOAl, repairs DNA single-strand breaks with damaged 3'-phosphate and 3'-phosphoglycolate ends. *Nucleic Acids Res*, 35: 3797-3809, 2007.
21. David-Cordonnier, M. H., Boiteux, S., and O'Neill, P. Excision of 8-oxoguanine within clustered damage by the yeast OGG1 protein. *Nucleic Acids Res*, 29: 1107-1113, 2001.
22. 杉本敏夫、東野義之、南 武志他。ケアマネジメント用語辞典 ミネルバ書房、京都、P109-P110, 2007
23. Valdmanis, P. N., Daoud, H., Dion, P. A., and Rouleau, G. A. Recent advances in the genetics of amyotrophic lateral sclerosis. *Curr Neurol Neurosci Rep*, 9: 198-205, 2009.
24. Martin, L. J. Neuronal cell death in nervous system development, disease, and injury. *Int*